Warm up of automotive catalyst substrates: comparison of measurements with predictions

Benjamin, S.F. and Roberts, C.A.

Original citation & hyperlink:
Benjamin, S.F. and Roberts, C.A. (1998) Warm up of automotive catalyst substrates: comparison of measurements with predictions. International Communications in Heat and Mass Transfer, volume 25 (1): 19–32.
http://dx.doi.org/10.1016/S0735-1933(97)00134-6

DRAFT SENT TO CONSORTIUM

WARM UP OF AUTOMOTIVE CATALYST SUBSTRATES: COMPARISON OF MEASUREMENTS WITH PREDICTIONS

S. F. Benjamin and C. A. Roberts
School of Engineering, Coventry University, UK

ABSTRACT

An understanding of the warm up of automotive catalysts is important for accurate prediction of light off. This work describes some experimental studies on warm up in the absence of chemical reactions. In parallel with these experiments, the temperatures of the warmed substrate have been predicted. The problem of warm up is a simple one, capable of analytical description, but since the complete problem of catalyst performance with chemical reactions will ultimately require CFD coding, the simple case is dealt with in this way to form the basis of a more complete model. The studies have found measured heat transfer coefficients which are in the range 15 to 20 W/(m^{2}K) for metallic substrates with sinusoidal channels. This is much lower than standard Nu values suggest. The predictions have also illustrated the significance of the heat transfer coefficient in obtaining accurate agreement with measurements in the simple case of warm up.

Introduction

An automotive catalyst substrate is placed in the exhaust system of an automobile as a support for the precious metal loading which acts catalytically on the exhaust gases to reduce pollutants. The simplest substrates, consisting of multiple parallel channels, can be either ceramic or metallic. A ceramic substrate is a monolithic matrix of cells, with each cell usually square in cross section, through which the gases pass. The cell side length is about 1 mm and cell density is in the range 46.5 to 77.5 cells/cm^2 (300 to 500 cpsi). The metallic substrates are composed of metal foil and corrugated metal foil wound together so that multiple parallel channels are formed, typically 62 cells/cm^2 (400 cpsi), with each channel having one approximately straight wall and one with sinusoidal form. In use, both types of substrate are washcoated with alumina/ceria which supports the precious metal, and the ceramic substrate is surrounded by a mat at the outer wall. Metal substrates are confined within a cylindrical metal mantle.

Catalyst warm up is of interest because of the phenomenon of light-off. The warming of the substrate is caused by the passage of exhaust products from the engine through the initially cold substrate. A critical temperature, about 250° C, is necessary on the substrate surface before the chemical reactions take off and warm the substrate

further to its optimum operating temperature. Ultimately, it would be desirable for the automotive industry to be able to simulate all the processes within the supply pipework and the catalyst structure. This would be a valuable design tool. A full simulation in the catalyst would encompass fluid flow, heat transfer, mass transfer and chemical kinetics on a channel by channel basis throughout the structure. To achieve this is not, however, at present computationally realistic. An alternative approach has been to model the catalyst as an equivalent porous medium [1] with bulk properties for flow resistance, thermal conductivity etc. With this approach, heat transfer between the gas and the solid within the substrate is described by heat transfer coefficients. Using this approach, full CFD predictions can be made for chemically active catalyst systems and can give good qualitative descriptions of their warm up behaviour, although quantitative agreement with experimentally measured data is less good. Qualitative descriptions are useful to design engineers, but complete confidence in predictions will be realised only when there is quantitative agreement with experimental measurements. The work which is described in this paper has investigated quantitative agreement between predictions and measurements in the simplest case: warm up of a catalyst substrate by a constant mass flow of air. In the situations studied, chemical reactions do not occur but the temperature of the in-flowing air rises with time. This very simple case has been investigated experimentally for metal and ceramic substrates, washcoated and non washcoated, and substrate temperatures have been predicted using the commercial CFD package Star-CD to solve the heat conduction and energy equations.

In the studies described here, the air entering the substrate shows a ramped rise in temperature with time, reaching 500 K after about 60 secs. This approximates to warm up in a real system. Heat is convected to the solid substrate by the gas, and the gas is thereby cooled. The substrate conducts heat radially to the outer wall to an extent determined by the net radial thermal conductivity of the structure and by losses at the outer wall. The substrate also conducts heat axially to the cooler portions of the substrate downstream to an extent determined by the effective axial conductivity of the substrate. This latter effect is very small but is accounted for when using the CFD package to solve for temperatures. The problem overall is a simple one, and there have been some attempts to solve it analytically (for example, Heck et al., [2]) but ultimately a complete model including spatially variable heat transfer coefficients, reaction chemistry etc. is required. It is thus advantageous to solve the simple problem numerically with the CFD code so that it is later straightforward to add on the other more complex aspects of the model once the validation of the simple warm up case is complete.

Theoretical basis

The mathematical description of catalyst warm up has been the subject of much research, for example by Byrne and Norbury [3] who looked at the equations in some detail, but did not use the equations to make predictions. As a first approximation, the simple case being investigated here is a lumped capacitance problem; so an energy balance suggests

$$m_g' C_{pg} (T_{gi} - T_{go}) = m_w C_w (T_{wf} - T_{wi})/\Delta t \qquad (1)$$

But the flux at any particular point is convection controlled,

$$q = h\,A\,(T_g - T_w) \quad (2)$$

where T_g , the bulk gas temperature, and T_w are both functions of (z,t)

For an element of length Δz of the catalyst substrate in a short time interval Δt

$$T_{gm} = (T_{gi} + T_{go})/2 \text{ and } T_{wm} = (T_{wf} + T_{wi})/2 \quad (3)$$

Thus using T_{gm} for T_g and T_{wm} for T_w an estimated value for h can be found for any specified length element of substrate from

$$hA(T_{gm} - T_{wm}) = m_w C_w (T_{wf} - T_{wi})/\Delta t \quad (4)$$

Considering the special case of the inlet plane of the substrate and assuming T_{gi} is constant,

$$m_w C_w \frac{dT_w}{dt} = h\,A\,(T_{gi} - T_w) \quad (5)$$

The solution for this case is $T_w = T_{gi} - (T_{gi} - T_{wi}) \exp[-hAt/(m_w C_w)]$ (6)

This clearly shows the relative importance of the parameters h, A, m_w and C_w in the process of wall warm up, and these parameters will be equally important when T_{gi} is a function of time during warm up. An important aspect of the transient problem is that in the very early stages of warm up the gas flow is depleted of heat and cooled to ambient before it has completed its path through the substrate. The problem is more completely expressed in terms of two simultaneous heat conduction equations, in the gas and in the solid. The co-ordinate system is set up so that the substrate axis and flow are in +z direction. The conduction equation for the substrate wall for axially symmetric conditions is

$$(1-\varepsilon)\left[k_z \frac{\partial^2 T_w}{\partial z^2} + k_x \frac{\partial^2 T_w}{\partial x^2} + k_y \frac{\partial^2 T_w}{\partial y^2} \right] + h\,A_v\,(T_g - T_w) = \rho_w (1-\varepsilon) C_w \frac{\partial T_w}{\partial t} \quad (7)$$

The energy equation describing the gas is

$$\varepsilon k_g \frac{\partial^2 T_g}{\partial z^2} = \rho_g \varepsilon C_{pg} \left[\frac{\partial T_g}{\partial t} + U \frac{\partial T_g}{\partial z} \right] + h\,A_v\,(T_g - T_w) \quad (8)$$

The quantity A_v is the effective bulk value for the substrate, a value which is specified by manufacturers for their substrate materials.

The CFD program solves these equations simultaneously. Figure 1 shows a mesh diagram for the simple system. The problem is dealt with as a 2D axisymetric problem, so that the cylindrical geometry is represented by a wedge with symmetry planes on its largest two surfaces. In Figure 1, the lower part features a short length of unobstructed tube at inlet, of length 4 cells, followed by a block of porous medium which is analogous in performance to the multiple channels of the substrate, and finally a short length of unobstructed tube at outlet, of length 4 cells. The upper image represents the bulk solid. The inlet boundary condition is a constant and spatially uniform mass flow of gas with temperature rising with time. The outlet boundary is at atmospheric pressure. The heat loss to the surroundings is specified at the mantle (losses from the bulk solid only). The initial condition is that the system contains fluid at rest at 293K. The inlet (impinged) face of the solid substrate and the outlet face are adiabatic. The side walls of both wedges are symmetry planes. The flow resistance of the channels of the substrate

is modelled by the equivalent porous medium and the bulk solid is modelled separately but linked via the calculated heat flux to the fluid in the porous medium using the method outlined in a report by Clarkson [4].

FIG. 1

Mesh used for CFD simulation

For each run of the CFD model, input parameters are specified to quantify the case. The inlet mass flow rate is fixed; an equation describes the rise in temperature with time. The geometry of the substrate determines A_v. The material of the substrate determines C_w, which is a function of temperature. The porosity (ε) determines the bulk density $(1-\varepsilon)\,\rho_w$ and also influences the effective axial and radial conductivities for the bulk substrate so that $(1-\varepsilon)k_z$ is replaced by k_{ax} and $(1-\varepsilon)k_{x,y}$ are replaced by k_r in equation (7). Values can be input for Nu and D_h, from which a value for h can be evaluated on a cell by cell basis, or alternatively h can be specified as constant. The mantle wall is either adiabatic or loses heat to the surroundings by either natural or forced convection. Resistance of the substrate is dealt with as an analogous porous medium so that values for permeability coefficients α and β are entered corresponding to the equation

$$\frac{dP}{dz} = -\alpha U^2 - \beta U \qquad (9)$$

Typical values of input data are given in Table 1. The values for radial thermal conductivity were measured using a cylindrical heater through the core of a 118 mm diameter sample to warm it to steady state [5]; and the values for axial conductivity were calculated from sample porosity. The mass flow rate was 6.5g/s through a substrate of 5 cm diameter and 0.15m length. This corresponds to a Reynolds number in each channel of the

substrate of about 250. Thus the CFD simulation was fully laminar. Washcoated samples have 159 kg/m^3 (± 3.8%) of washcoat material (alumina/ceria with no precious metal) of density 1350 kg/m^3 applied to their surfaces.

TABLE 1
Input Data For CFD Simulation of Substrate Warm Up

	Metal 62 cell/cm^2	Ceramic 62 cell/cm^2	Ceramic wc 62 cell/cm^2
A_v (m^2/m^3)	3691	2770	2526
D_h (mm)	0.9758	1.108	1.019
C_{pw} (J/(kg K))	490	1100	1059
$(1-\varepsilon)\rho_w$ (kg/m^3)	708	420	579
k_{ax} (W/(mK))	1.39	0.34	0.36
k_r (W/(mK))	0.37	0.21	0.30
α	30	0.0001	0.0001
β	400	555	874
porosity ε	0.901	0.76	0.642

Initially, the value of Nu used for the metal substrate samples was 2.213, as quoted by Shah and London [6] for Nu(H1) for sinusoidal channels for an aspect ratio of 1/4 (peak to peak height /wavelength). For the ceramic substrates, a Nu value of 3.608 was used for square channels. The Nu value was elevated on a cell by cell basis to allow for increased heat transfer in the first few cells downstream of inlet to the channels. Heat transfer coefficient h is then calculated for the local temperature. The CFD simulation solves for temperature in the solid and the gas and for velocity in the fluid.

A Nu value of 2.213 corresponds to a heat transfer coefficient of 58 W/(m^{2}K) at 300 K and to a heat transfer coefficient of 89 W/(m^{2}K) at 500K. Experimental measurements, which are discussed below, have suggested an h value lower than this than this for much of the warm up period. Although initially higher in value, h *decreases* with time during the experiment so that it is lower at times when temperatures are higher. In later CFD simulations, h values based on these experimental observations have been used to improve agreement between measurements and predictions.

Description of the experimental test rig

The experimental test rig is shown schematically in Figure 2. Air from a compressed air supply is regulated to about 3 bar gauge pressure and discharged through a gate valve to the test rig. The air mass flow is monitored by a calibrated viscous flow meter downstream of the gate valve. The air enters a heating chamber containing nine 1 kW heating elements. Immediately downstream of the heating chamber is a honeycomb flow straightener and converging nozzle which supplies air with a uniform velocity profile to the 0.05m diameter substrate sample. The procedure for start up is to heat the chamber for 90 secs. before turning on the air. This gives a temperature rise with time which is an acceptable approximation to temperature rise in warming exhaust systems. The system is

mounted so that the air is ducted downwards; this avoids buoyancy problems which distort the inlet temperature profiles if the system is mounted horizontally.

FIG. 2

Schematic diagram of experimental test rig

The temperature of the inlet and exhaust air is monitored with thermocouples. The substrate samples are drilled with 0.7 mm (28 thou) diameter holes to allow insertion of fine wire thermocouples into the sample for measurement of substrate wall temperatures. The thermocouples used were K type of 0.5 mm diameter with 0.025 s response time. The insertion of each thermocouple significantly obstructs the gas flow in the channel which accommodates the tip. Furthermore, the tip of each thermocouple is treated with a speck of heat conducting paste to improve contact with the wall. The thermocouple is also taped to the supports of the test rig in such a way that its tip is forced against the substrate wall. The measurements recorded by the thermocouples are therefore assumed to be representative of wall temperatures.

The holes for the thermocouples are drilled radially to the specified depth, but successively in a spiral along the length of the substrate sample, so that each thermocouple tip probes the wall of a previously unobstructed channel. Temperatures recorded during warm up are logged by a PC based system and so are directly available for analysis.

Results

Experimental measurements of heat transfer coefficient

Measurements were made of heat transfer coefficient by application of equation (4). Local gas temperature was deduced from the gas inlet temperature and the gas exit temperature by linear interpolation. This is inaccurate at

low times, but is valid after about 35 secs. in the cases studied. An assumption was made that the significant transfer of heat to any element of the wall was by convection from the gas, but that transfer was negligible by conduction from adjacent solid elements. Simulations have been run to investigate this under conditions similar to those of the experiments. It has been shown that increasing axial conductivity in simulations to about four times its real value does not change the predicted temperatures and so clearly axial conductivity does not have a significant effect. The rate of rise of wall temperature locally was therefore assumed to give a measurement of convective flux to that element as a function of time. The results are shown plotted in Figures 3, 4 and 5.

FIG. 3

Measured h for 62 cells/cm^2 metal sample

FIG. 4

Measured h for 75 cell/cm^2 metal sample

FIG. 5

Measured h for 46.5 cells/cm^2 sample

The three plots are for metal substrates with three different cell densities, 46.5, 62 and 77.5 cells/cm^2, all having sinusoidal channels and with approximate aspect ratios of 1/ 2.5, 1/ 3.6 and 1/2.6 respectively. Despite the scatter, it is clear that a feature common to the three plots is the trend towards a very low value, about 15 or 20 W/(m^2K), at high times. Peaks are observed at low times when the linear interpolation for gas temperature is inaccurate, that is below about 35 secs. This feature is present in all three figures. Interestingly, any attempt to correct the local gas temperatures at low times would make the value of ($T_g - T_w$) smaller and the values found for h would then be correspondingly higher. These are preliminary results, but have influenced the choice of h value for use in the CFD simulations. A value near 30 W/(m^2K) is now routinely used for simulations for the 62 cell/cm^2 non washcoated metal catalyst substrate, rather than a value of 60 to 80 W/(m^2K) which had seemed the most reasonable value to use initially.

An inspection of Figures 3, 4 and 5 shows that measured heat transfer coefficient is apparently time dependent. It is more likely, however, that it depends on the temperature and flow conditions, as can be argued from the following simple analysis. The heat transferred expressed as a convective flux to the wall is h A ($T_g - T_w$), assuming that T_g is representative of the bulk temperature of the gas. Also, the heat transferred can be expressed as a flux conducted through the layer of gas adjacent the wall from the bulk of the gas. That flux is $|k_g A (T_g - T_w)/b|$, where b is the thickness of the layer between gas at the bulk temperature and the wall. Thus heat transfer coefficient h is equal to (k_g/b). The variation of k_g with temperature, and hence with time, is known. The variation of b with time in a spatially developing and/or thermally transient situation may not be known. This simple analysis, however, suggests a minimum value for h when b is approximately equal to the channel half-width. For

example, at 300K, k_g is 0.0262 W/(mK) and if channel half-width is 0.0005m, then h (minimum) is 52.4 W/(m^2K) whereas at 500 K, k_g is 0.0404 W/(mK) and h (minimum) is 80.8 W/(m^2K). Thus the deduced minimum h value increases with temperature whereas experimental observations show h decreasing with time and temperature to much lower values.

Comparison of CFD simulations with measured wall temperatures

A comparison of measurements and CFD predictions for a non washcoated 62 cell/cm^2 ceramic sample is shown in Figure 6. The location indicated on the abscissa is measured in the axial direction from the inlet to the substrate. A fairly steep fall off of temperature along the length of the substrate is noted. Agreement between measurements and predictions is fair, with temperatures under predicted in the first 20 seconds of warm up and over- predicted at 40 seconds.

FIG. 6
Comparison of measured and predicted temperatures for non washcoated ceramic substrate

FIG. 7
Comparison of measured and predicted temperatures for washcoated ceramic substrate

FIG. 8
Comparison of measured and predicted temperatures for non washcoated metal substrate

Figure 7 shows results for a washcoated 62 cell/cm^2 ceramic sample. The effect of the additional mass can be noticed when Figure 7 is compared with Figure 6. There is a steeper fall off of temperature along the length of the substrate, which is correctly predicted. Again, agreement between measurements and predictions is fair, but temperatures are under predicted in the early stages of warm up with better agreement by 40 seconds. In the case of the ceramic substrates, Figures 6 and 7, the heat transfer coefficient used for the CFD predictions was found from Nu of 3.608 using local values of the thermal conductivity of air. The h value deduced was elevated over the first five computational cells (cell length 2.5 mm) by factors of 1.9, 1.5, 1.2, 1.15 and 1.1 to make an allowance for inlet effects. This is an arbitrary correction, based approximately on the standard ratio Nu_d/Nu_∞ for the thermal entry region of a circular tube with laminar flow [7].

Figure 8 shows a typical set of results for a 62 cells/cm^2 non washcoated metal sample, and the values for substrate temperatures predicted by the CFD simulation. Agreement is seen to be reasonably good, but there is under prediction of wall temperatures at low times with closer agreement at later times, 40 to 60 secs. Over prediction of wall temperatures is observed if simulations are extended to longer times. A less steep fall off of temperature along the length of the tube is noted in the measurements, when compared with the ceramic substrates, and this is predicted. The predicted substrate temperatures in Figure 8 were found by fixing h at a constant value 30 W/(m^{2}K), which is low, except over the first five cells at inlet where its value was elevated arbitrarily by higher factors of 3.8, 2.63, 1.8, 1.44, and 1.1. This gave values at inlet closer to those which would have been obtained using an h value of 58 W/(m^{2}K), as discussed earlier, together with the Nu_d/Nu_∞ ratio referred to above.

Figure 9 shows predicted substrate temperatures from simulations using various values for h: 5, 30 and 60 $W/(m^2K)$. The value for h of 5 $W/(m^2K)$ was elevated by factors of 22.8, 11.4, 5.7, 2.9, and 1.4; the value for h of 30 $W/(m^2K)$ was elevated by factors of 3.8, 2.63 etc. and for h of 60 $W/(m^2K)$ by factors of 1.9, 1.5 etc. over the first five cells. These arbitrary elevations gave similar values near the inlet in all cases. Figure 9 shows very clearly the influence which the value of h has on the temperature predictions from simulations. A change from 30 to 60 $W/(m^2K)$ had a negligibly small effect on predicted gas temperature and so these have been plotted as a single line for clarity.

FIG. 9

Effect of h on predictions for 62 cell/cm^2 metal substrate

FIG. 10

Measured substrate temperatures compared with predictions using alternative forms for h

Figure 10 shows a comparison of some measurements made for a lower flow rate, 4.9 g/s, in a 62 cell/cm^2 non washcoated metal substrate. Two alternative predictions are shown. In one case h is a nominally constant 30 W/(m^{2}K), with the values elevated by 3.8, 2.63 etc. over the first five cells. In the other case, influenced by the observation of low h values in the experiments, the value of h was input as data on a cell by cell basis with the following values: 200, 170, 120, 80, 50, 35, 25 and 20 W/(m2K) in the first nine cells respectively and a constant 15 W/(m^{2}K) thereafter. The latter prediction does show very good agreement with the shape of the measured temperature curves in the inlet region and demonstrates the way that variation of h with location can improve the fit of the CFD predictions to the observed temperatures in the inlet region. There is still, however, a problem of under prediction at low times which cannot be solved at this stage by simple adjustment of a time independent heat transfer coefficient.

Conclusions

Preliminary indications are that the heat transfer coefficient for use in a metallic catalyst substrate with sinusoidal channels has a lower value than would be indicated by use of standard Nu number data. Typical values observed in experiments after 60 secs. of warm up are 15 to 20 W/(m^{2}K). At earlier times values are higher and there is also evidence of different values at different locations within the substrate.

Measurements have been compared with predictions for ceramic substrates, washcoated and non washcoated, and for a non washcoated 62 cell/cm^2 metal substrate. Agreement between full simulations and measured substrate wall temperatures are fair for the ceramics, with good prediction of the way washcoat affects the temperature gradient along the substrate length. In the case of the metal, agreement is reasonably good, although there are discrepancies at low times and at high times with best agreement over the range 40 to 60 secs. Temperatures are generally under predicted at low times; the substrate warms up faster than predicted in the first 20 or 30 secs.

It seems unlikely that a universally constant value for heat transfer coefficient can be used to describe transient warm up of automotive catalyst substrates. The work described here has, however, provided useful insights into values which should be used. This will help to provide the basis for a more complete engineering model, which will provide accurate predictions only when warm up prior to light off is accurately predicted. The values presented in this paper would suggest that a value for h of 15 to 20 W/(m^{2}K) should be used for metallic substrates with sinusoidal channels, but with some allowance being made for elevation of this value just downstream of the channel inlet.

Future Work

The work reported here has been essentially one dimensional, as mass flows have been uniform across the substrate and measurements have been made at radial depths well away from the wall where there is no influence of the thermal losses at the mantle. Work is continuing on the effects of the washcoat layer and also on larger

diameter samples which are used in practical exhaust systems. With the larger samples, usually 118 mm diameter, a conical expander or a sudden expansion is placed between the supply nozzle and the substrate. Thus, even when the 50 mm diameter nozzle supplies uniform mass flow and temperature profile, these quantities will not be uniform at inlet to the substrate. Work has been reported on predicting velocity profiles at inlet to the substrate in similar geometries with cold flow [8]. The extension of the work reported here will aim to predict wall temperatures in the substrate using temperature and mass flow information upstream of the expander as the inlet boundary condition. A two dimensional distribution of temperature, i.e. T(r,z), will then be observed by measuring at different radial depths within the substrate. Measurements and predictions will be compared and it is anticipated that as in the work described here, a crucial decision for obtaining agreement between measurements and predictions will be the choice of value for heat transfer coefficient.

Acknowledgements

The authors acknowledge Jaguar Cars Ltd., Ford, Johnson Matthey and Arvin Cheswick International, whose generous financial support, technical advice, provision of catalyst substrate samples and other hardware have enabled this work to proceed.

Nomenclature

A	wetted surface area (m^2)
A_v	wetted surface area per unit bulk volume of substrate (m^2/m^3)
C_{pg}	specific heat of gas (J/(kg K))
C_w	specific heat of substrate wall material (J/(kg K))
D_h	hydraulic diameter of a single channel of substrate
h	heat transfer coefficient ($W/(m^2K)$)
k_g	thermal conductivity of gas (W/(mK))
k_{ax}	effective axial thermal conductivity of bulk substrate (W/(mK))
k_r	effective radial thermal conductivity of bulk substrate (W/(mK))
$k_{x,y,z}$	thermal conductivity of substrate wall material (W/(mK))
m_g'	mass flow rate of gas (kg/s)
m_w	mass of substrate wall (kg)
Nu	Nusselt number (dimensionless heat flux)
P	pressure (Pa)
q	heat flow rate (J/s)
r	radial depth (m)
t	time (s)
Δt	time interval (s)
T_g	temperature of gas (K)

T_w	temperature of substrate wall (K)
T_{gi}	temperature of gas at inlet to substrate (K)
T_{go}	temperature of gas at outlet from substrate(K)
T_{wi}	initial temperature of substrate wall (K)
T_{wf}	final temperature of substrate wall (K)
T_{gm}	mean temperature of gas (K)
T_{wm}	mean temperature of substrate wall (K)
U	velocity of gas flow (in z direction) (m/s)
x, y, z	Cartesian co-ordinates
α, B	permeability coefficients [kg/m4 and kg/(m3 s) respectively]
ε	porosity (fraction)
ρ_w	density of material of substrate walls (kg/m3)
ρ_g	density of gas (kg/m3)

References

1. R. J. Clarkson, S. F. Benjamin, T. S. Jasper and N. S. Girgis, SAE Technical Paper Series 931071, Proc I Mech E /SAE Vehicle Thermal Management Systems Conference, Ohio (1993)

2. R. H. Heck , J. Wei and J. R. Katzer , Chemical Reaction Engineering II p34 (1974)

3. H. Byrne and J. Norbury , Math. Engng. Ind. 4 p27 (1993)

4. R. J. Clarkson, Computational Dynamics Ltd. Report CD96/999/R4 (1996)

5. S. F. Benjamin, E. G. W. Day, N. S. Girgis, N. Haimad and C. A. Roberts, An Experimental and Theoretical Investigation of the Warm Up of Automotive Catalysts, Coventry University Internal Progress Report (Nov 1995)

6. R. K. Shah and A. L. London, *Laminar Flow Forced Convection in Ducts,* pp 253-256 Publ. Academic Press Inc. (1978)

7. J. P. Holman, *Heat Transfer,* p290 Seventh Edition Publ. McGraw-Hill, UK (1992)

8. S. F. Benjamin, R. J. Clarkson, N. Haimad and N. S. Girgis, SAE Technical Paper Series 961208, Int. Spring Fuels and Lubricants Meeting, Michigan (1996)

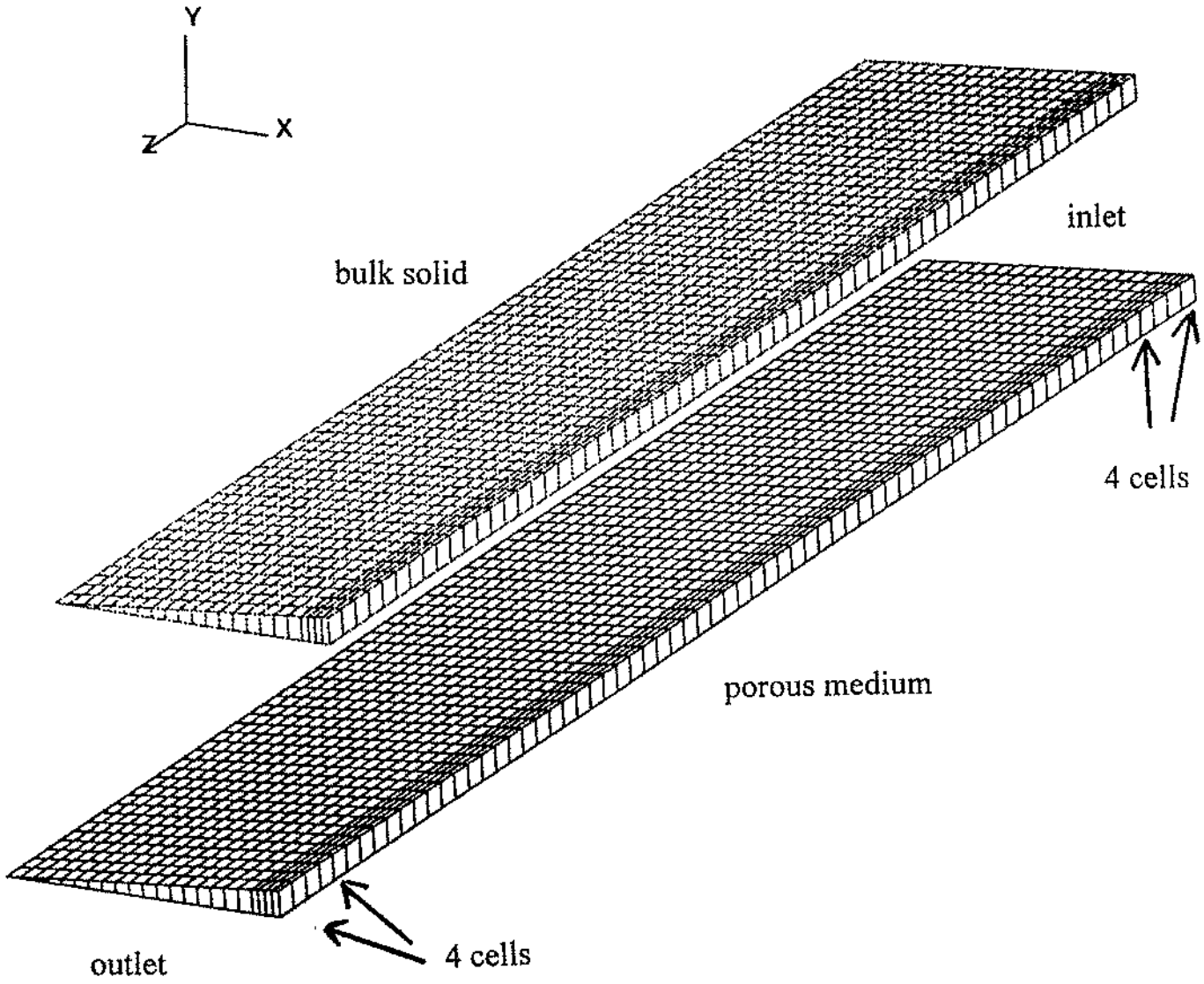

FIG. 1

FIG. 2

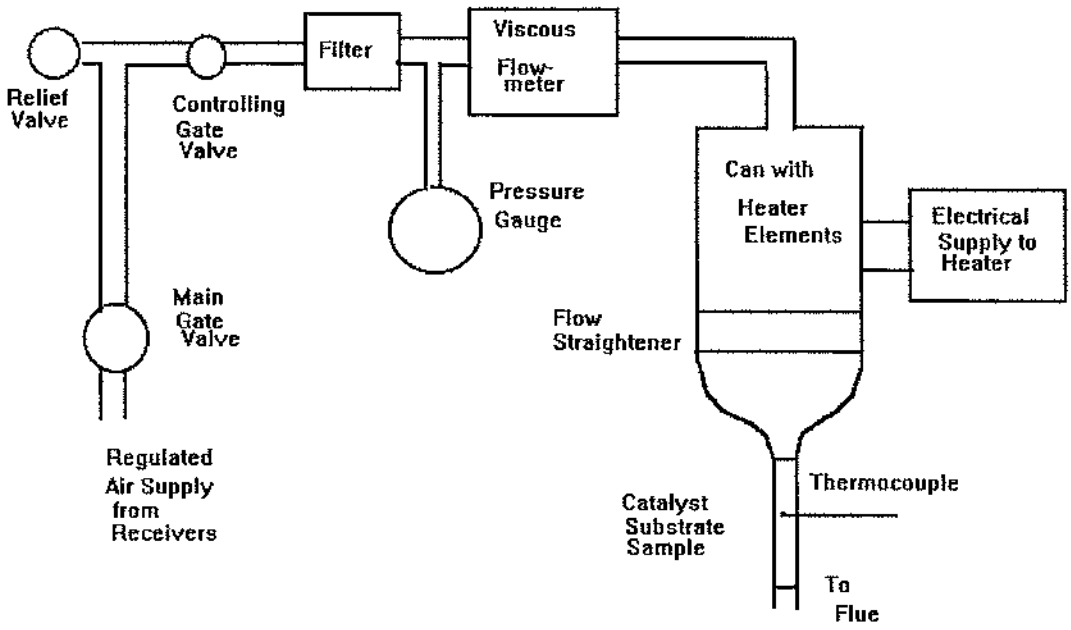
Relief Valve
Controlling Gate Valve
Filter
Viscous Flow-meter
Pressure Gauge
Can with Heater Elements
Electrical Supply to Heater
Main Gate Valve
Flow Straightener
Regulated Air Supply from Receivers
Thermocouple
Catalyst Substrate Sample
To Flue

FIG. 3

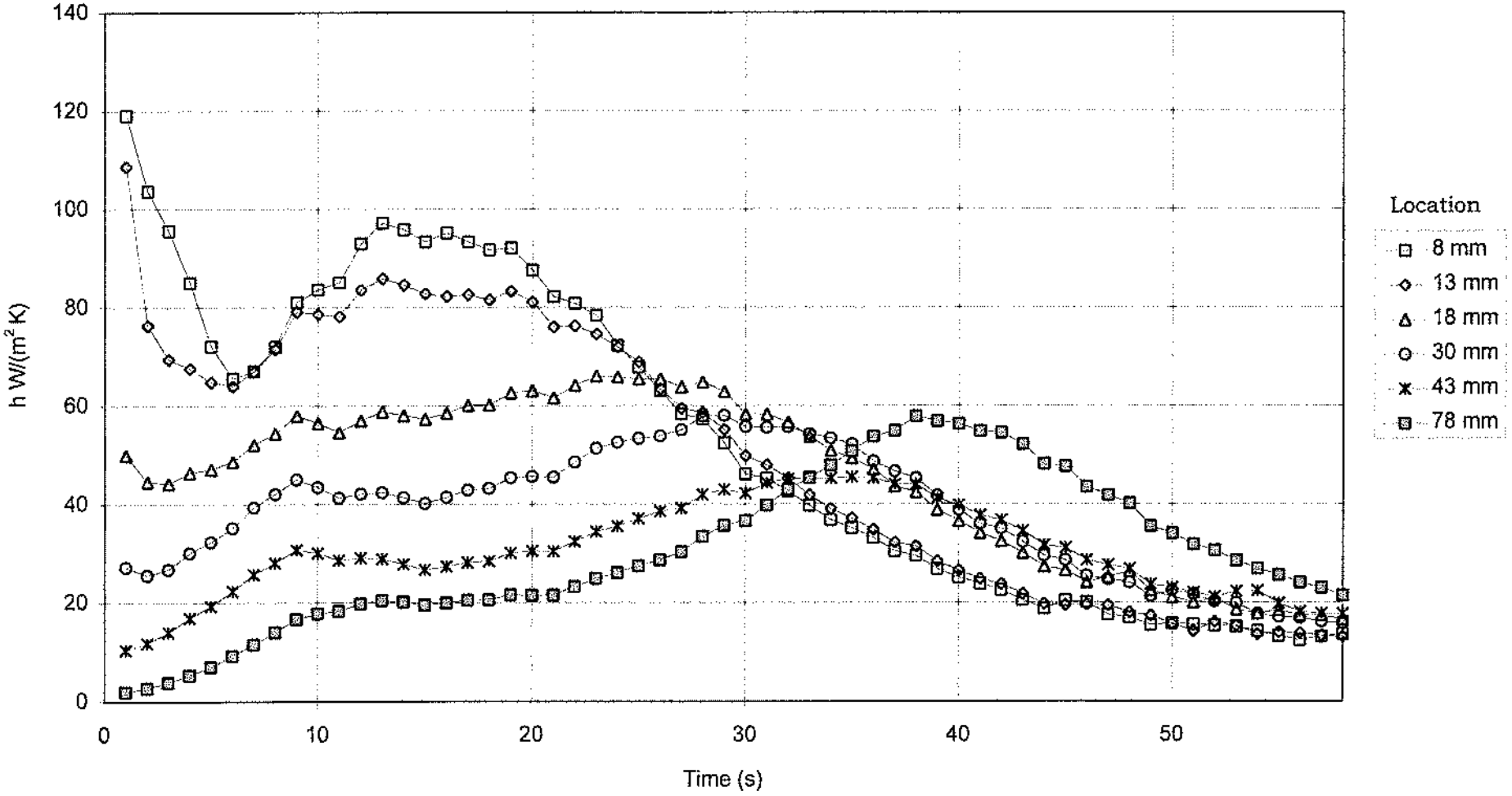
140
120
100
80
60
40
20
0
h W/(m² K)
0
10
20
30
40
50
Time (s)
Location
8 mm
13 mm
18 mm
30 mm
43 mm
78 mm

FIG. 4

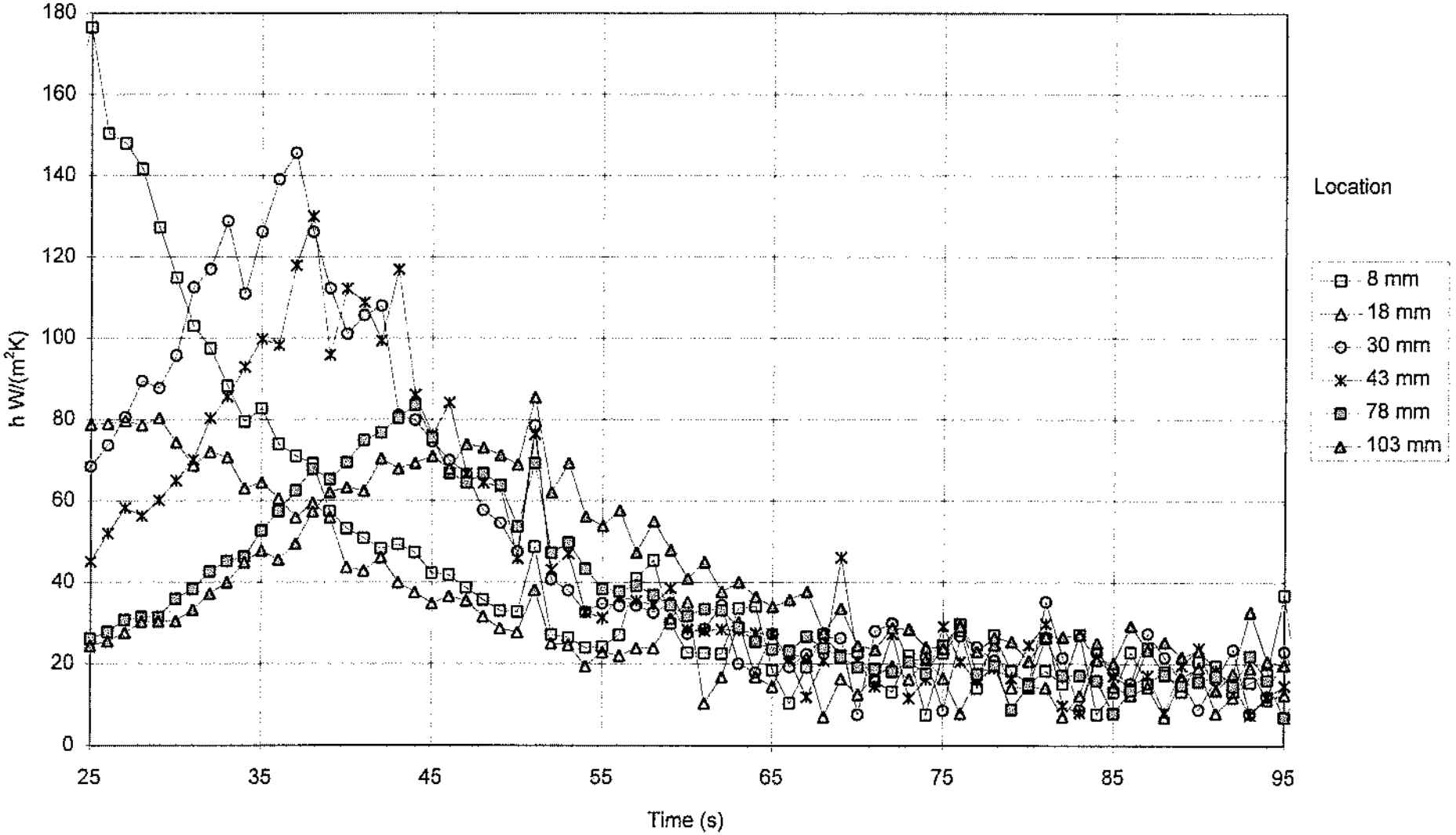
h W/(m²K)
180
160
140
120
100
80
60
40
20
0
25
35
45
55
65
75
85
95
Time (s)
Location
8 mm
18 mm
30 mm
43 mm
78 mm
103 mm

FIG. 5

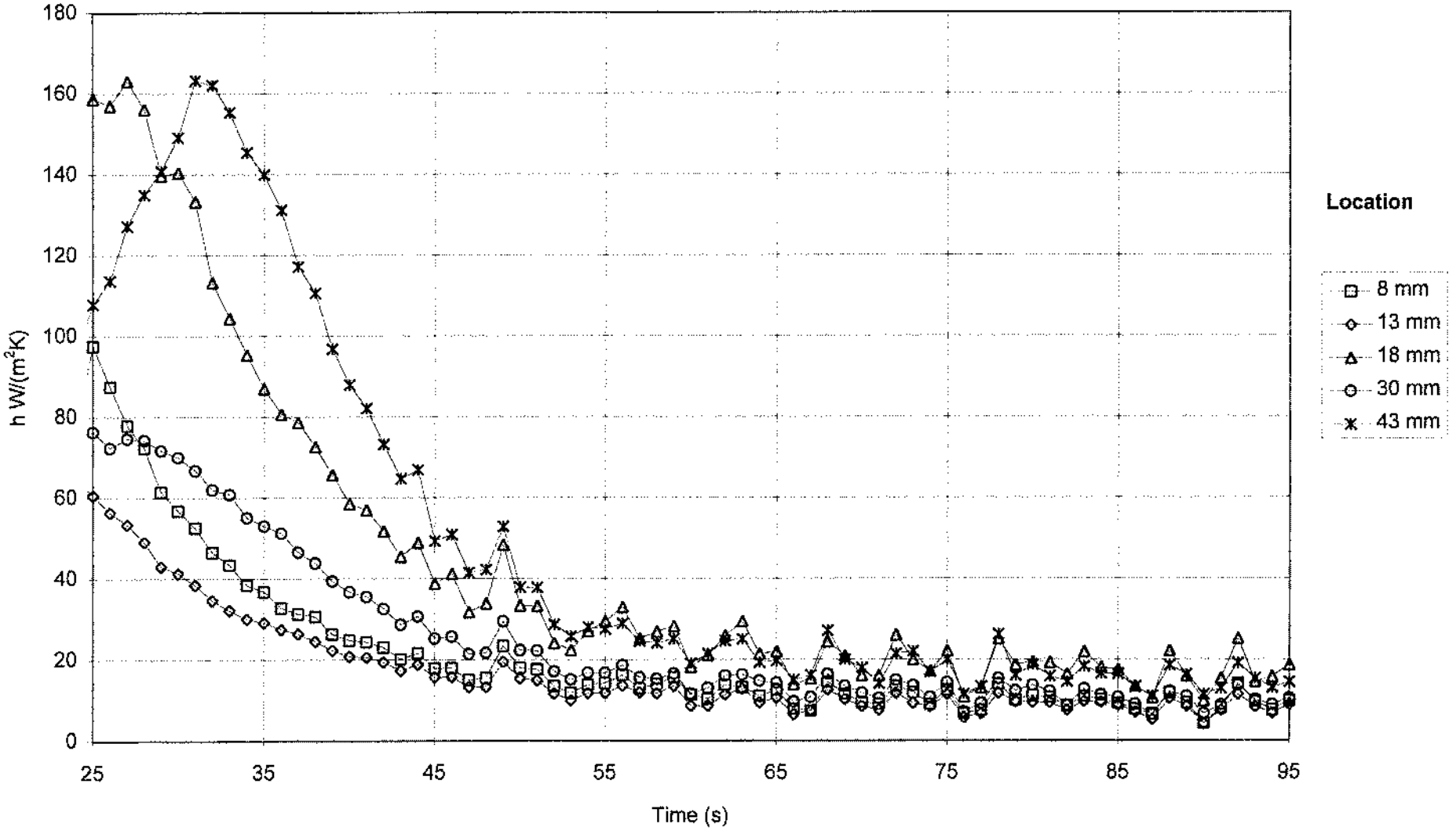
180
160
140
120
100
80
60
40
20
0
h W/(m²K)
25
35
45
55
65
75
85
95
Time (s)
Location
8 mm
13 mm
18 mm
30 mm
43 mm

FIG. 6

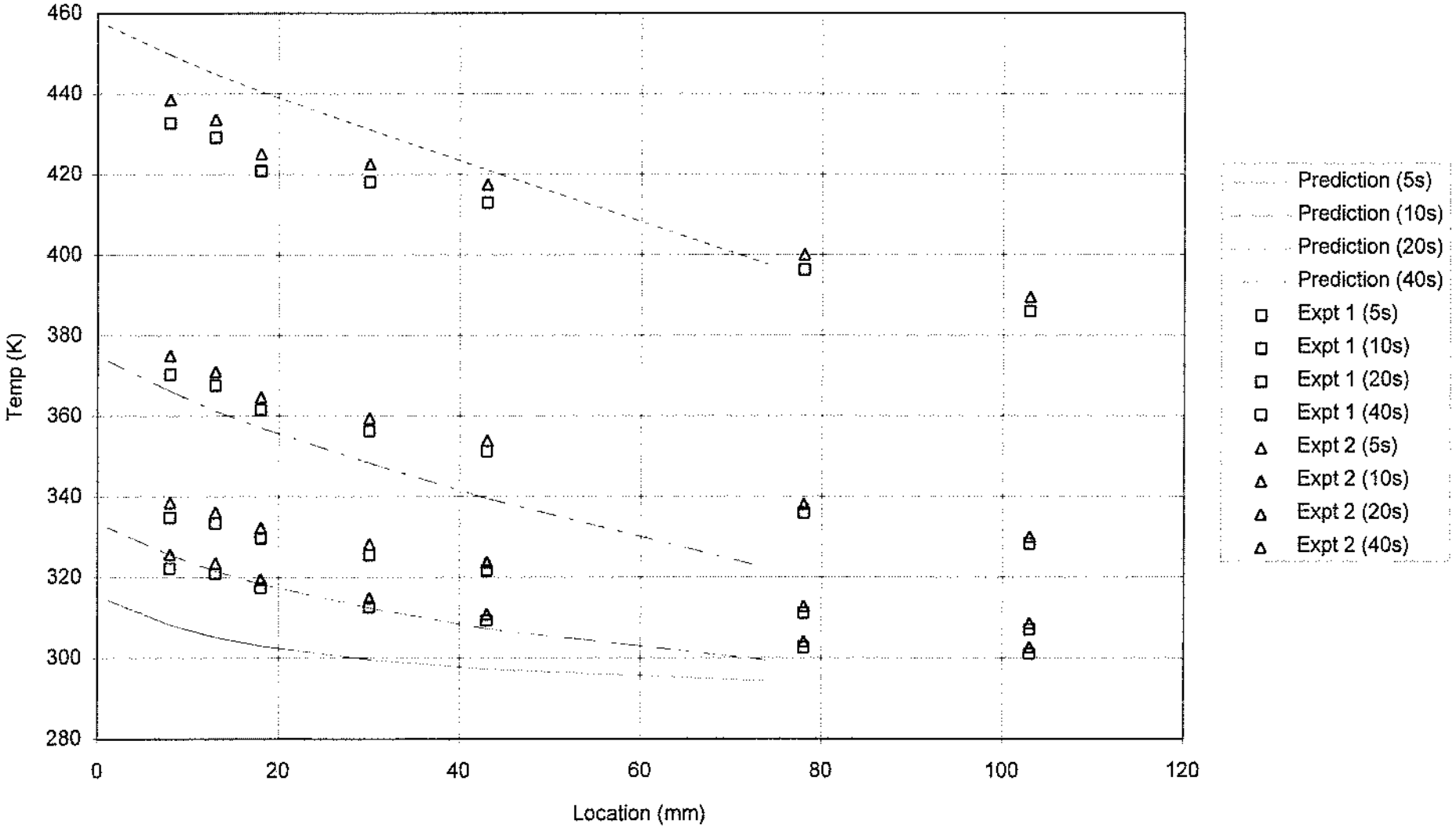
460
440
420
400
380
360
340
320
300
280
Temp (K)
0
20
40
60
80
100
120
Location (mm)
Prediction (5s)
Prediction (10s)
Prediction (20s)
Prediction (40s)
Expt 1 (5s)
Expt 1 (10s)
Expt 1 (20s)
Expt 1 (40s)
Expt 2 (5s)
Expt 2 (10s)
Expt 2 (20s)
Expt 2 (40s)

FIG. 7

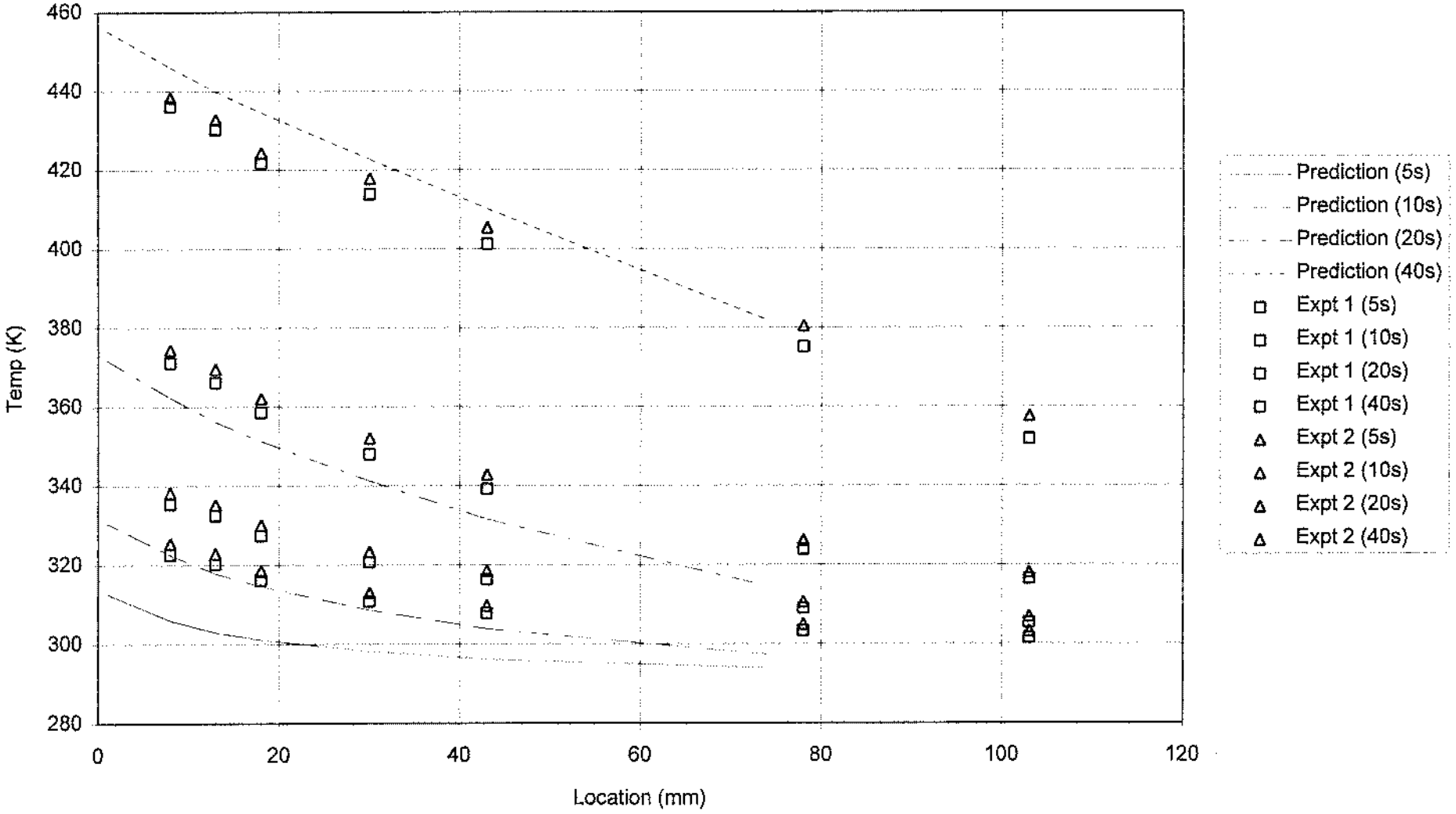
460
440
420
400
380
360
340
320
300
280
Temp (K)
0
20
40
60
80
100
120
Location (mm)
Prediction (5s)
Prediction (10s)
Prediction (20s)
Prediction (40s)
Expt 1 (5s)
Expt 1 (10s)
Expt 1 (20s)
Expt 1 (40s)
Expt 2 (5s)
Expt 2 (10s)
Expt 2 (20s)
Expt 2 (40s)

FIG. 8

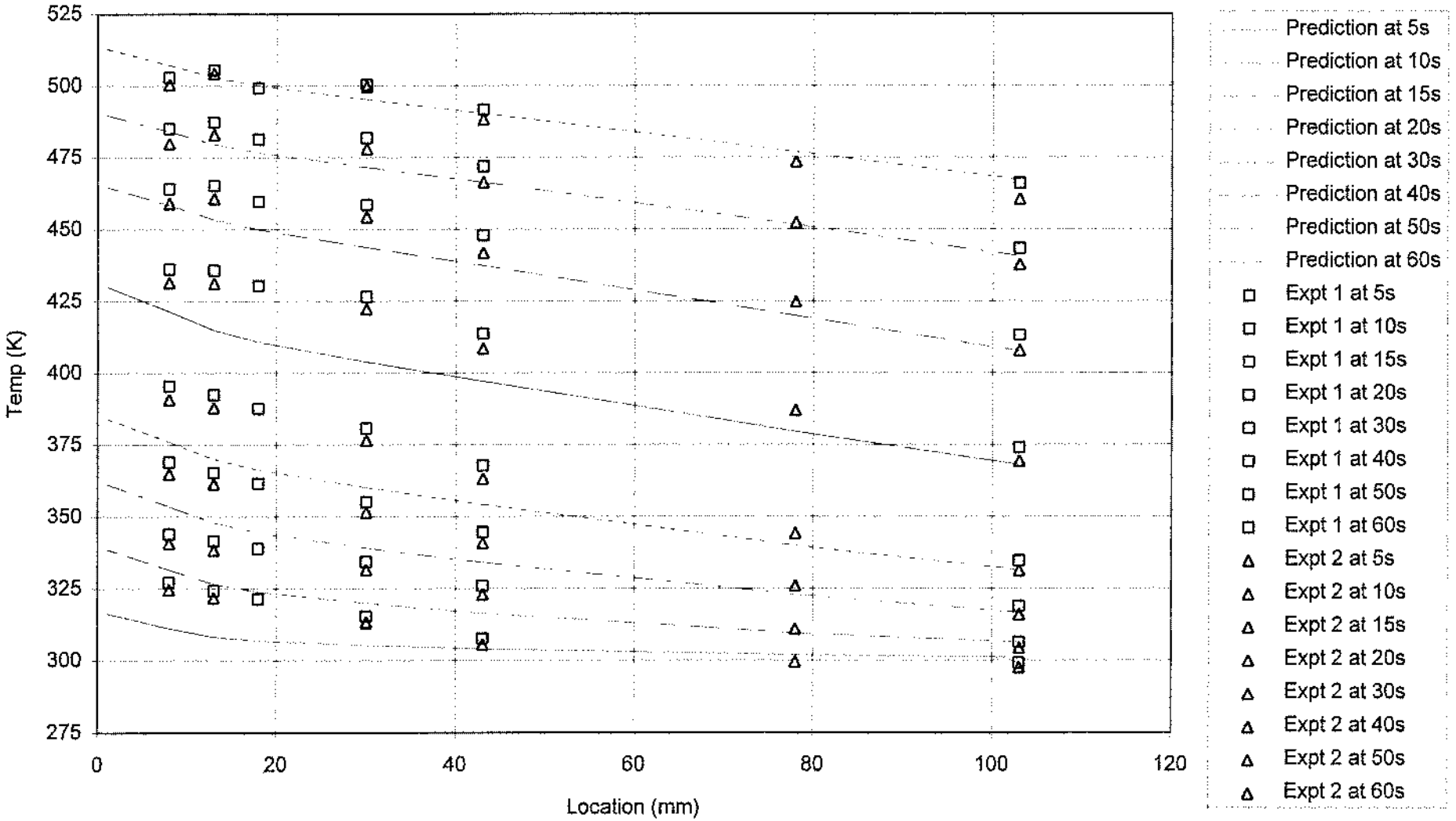
525
500
475
450
425
400
375
350
325
300
275
Temp (K)
0
20
40
60
80
100
120
Location (mm)
Prediction at 5s
Prediction at 10s
Prediction at 15s
Prediction at 20s
Prediction at 30s
Prediction at 40s
Prediction at 50s
Prediction at 60s
Expt 1 at 5s
Expt 1 at 10s
Expt 1 at 15s
Expt 1 at 20s
Expt 1 at 30s
Expt 1 at 40s
Expt 1 at 50s
Expt 1 at 60s
Expt 2 at 5s
Expt 2 at 10s
Expt 2 at 15s
Expt 2 at 20s
Expt 2 at 30s
Expt 2 at 40s
Expt 2 at 50s
Expt 2 at 60s

FIG. 9

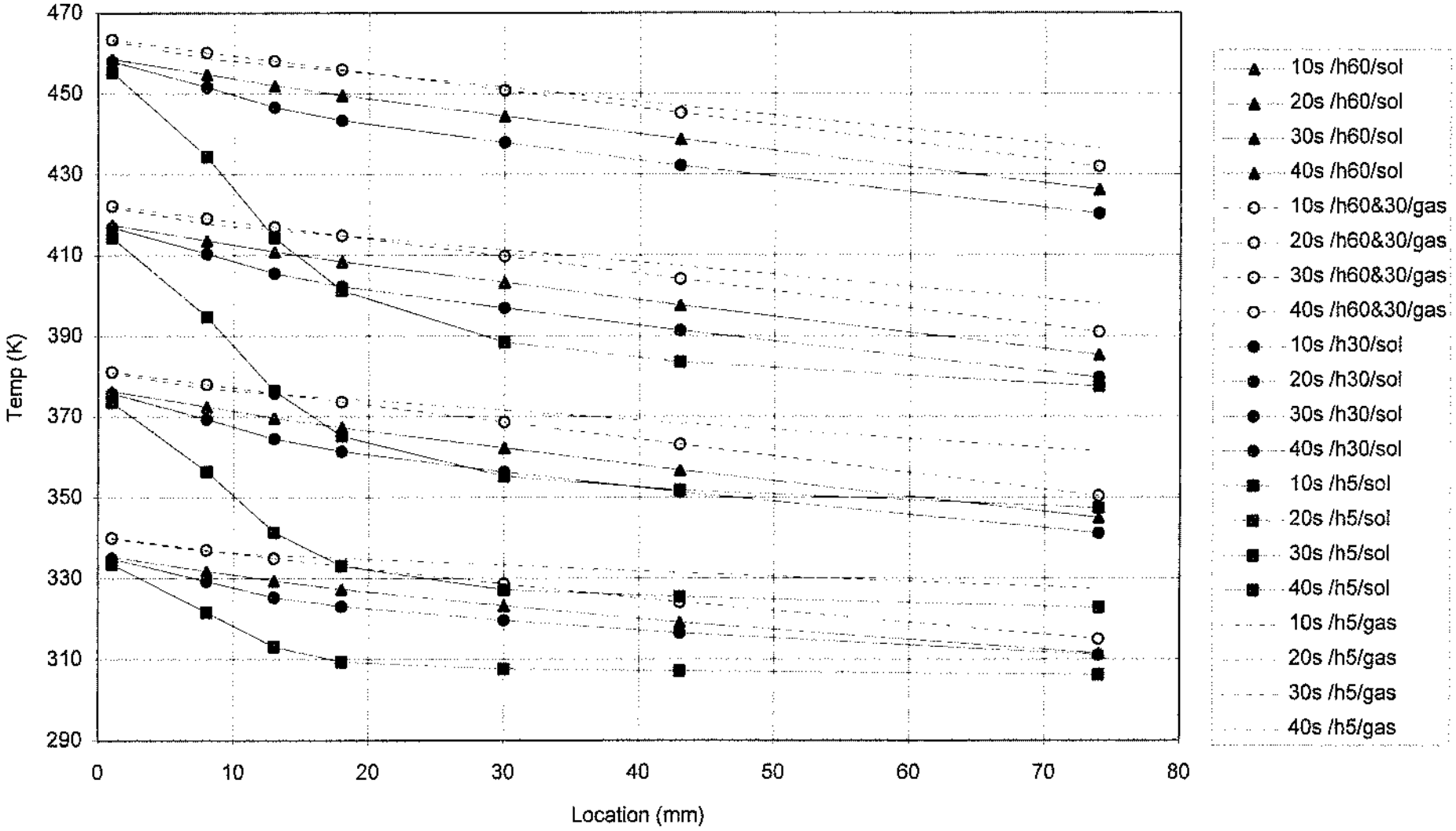
Temp (K)
470
450
430
410
390
370
350
330
310
290
0
10
20
30
40
50
60
70
80
Location (mm)
10s /h60/sol
20s /h60/sol
30s /h60/sol
40s /h60/sol
10s /h60&30/gas
20s /h60&30/gas
30s /h60&30/gas
40s /h60&30/gas
10s /h30/sol
20s /h30/sol
30s /h30/sol
40s /h30/sol
10s /h5/sol
20s /h5/sol
30s /h5/sol
40s /h5/sol
10s /h5/gas
20s /h5/gas
30s /h5/gas
40s /h5/gas

FIG. 10

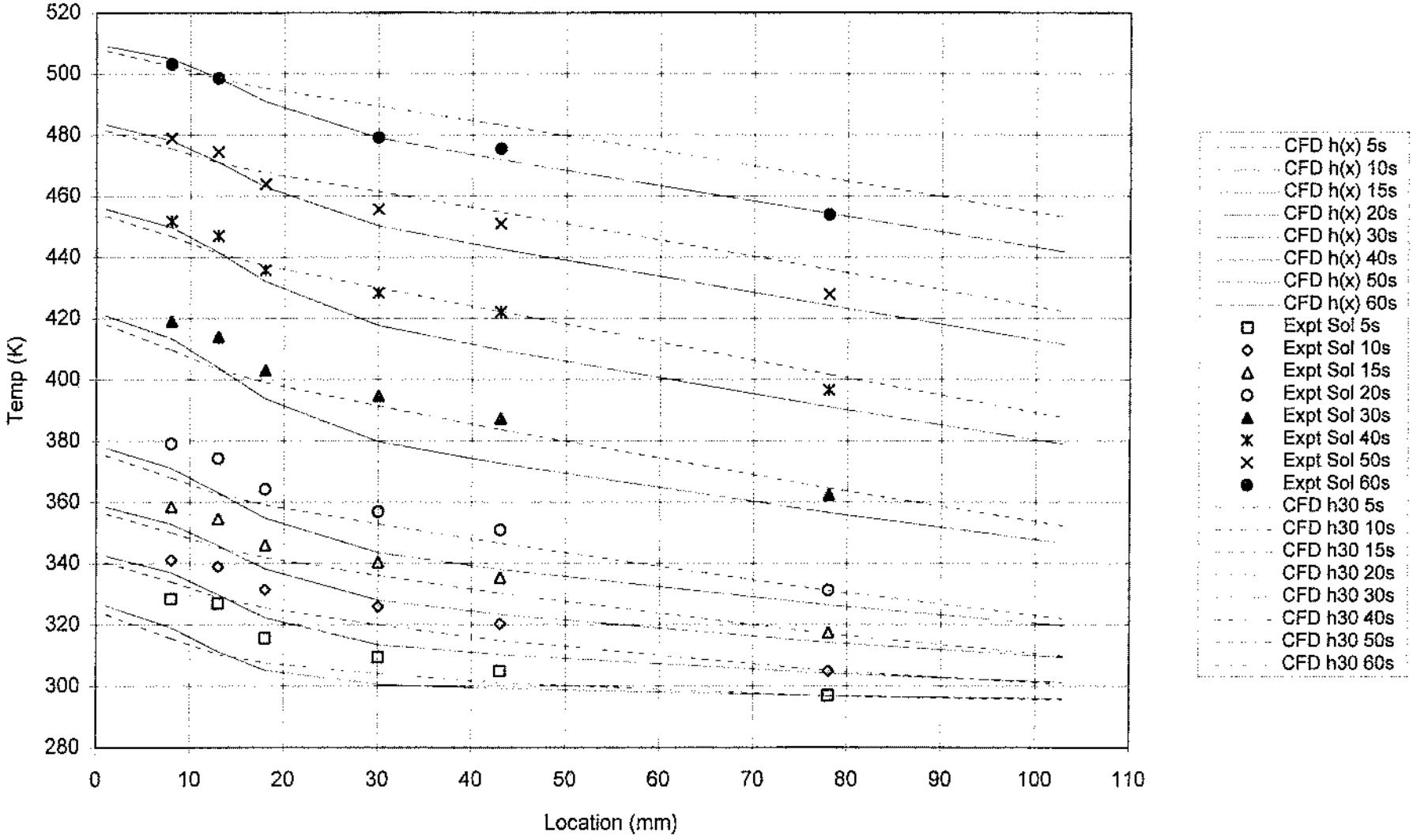
Temp (K)
520
500
480
460
440
420
400
380
360
340
320
300
280
0
10
20
30
40
50
60
70
80
90
100
110
Location (mm)
CFD h(x) 5s
CFD h(x) 10s
CFD h(x) 15s
CFD h(x) 20s
CFD h(x) 30s
CFD h(x) 40s
CFD h(x) 50s
CFD h(x) 60s
Expt Sol 5s
Expt Sol 10s
Expt Sol 15s
Expt Sol 20s
Expt Sol 30s
Expt Sol 40s
Expt Sol 50s
Expt Sol 60s
CFD h30 5s
CFD h30 10s
CFD h30 15s
CFD h30 20s
CFD h30 30s
CFD h30 40s
CFD h30 50s
CFD h30 60s